Determination of transverse momentum dependent gluon density from HERA structure function measurements

Hannes Jung[1,2], *Francesco Hautmann*[3]

[1]DESY, Notkestraße 85, 22607 Hamburg, Germany
[2]CERN, 1211 Genève 23, Switzerland
[3]Theoretical Physics Department, University of Oxford, Oxford OX1 3NP, GB

DOI: `http://dx.doi.org/10.3204/DESY-PROC-2012-02/29`

The transverse momentum dependent gluon density obtained with CCFM evolution is determined from a fit to the latest combined HERA structure function measurements.

1 Introduction

The combined measurements of the structure function at HERA [1] allow the determination of parton distribution functions to be carried out to high precision. While these data have been used to determine the collinear parton densities, the transverse momentum distributions (TMD) or unintegrated gluon distributions were only based on older and much less precise measurements [2, 3].

In high energy factorization [4] the cross section is written as a convolution of the partonic cross section $\hat{\sigma}(k_t)$ which depends on the transverse momentum k_t of the incoming parton with the k_t-dependent parton density function $\tilde{\mathcal{A}}(x, k_t, p)$:

$$\sigma = \int \frac{dz}{z} d^2k_t \hat{\sigma}(\frac{x}{z}, k_t) \tilde{\mathcal{A}}(x, k_t, p) \tag{1}$$

where p is the factorization scale. The evolution of $\tilde{\mathcal{A}}(x, k_t, p)$ can proceed via the BFKL, DGLAP or via the CCFM evolution equations. Here, an extension of the CCFM evolution is applied (to be also used in the parton shower Monte Carlo event generator CASCADE [5]) which includes the use of two loop α_s as well as applying a consistency constraint [6, 7, 8] in the $g \to gg$ splitting function [9]:

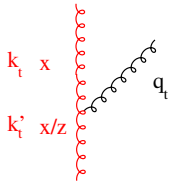

Figure 1: Gluon branching

$$P_{gg}(z, p, k_t) = \bar{\alpha}_s(k_t^2) \left(\frac{(1-z)}{z} + \frac{z(1-z)}{2} \right) \Delta_{ns} + \bar{\alpha}_s(p^2) \left(\frac{z}{1-z} + \frac{z(1-z)}{2} \right), \tag{2}$$

with Δ_{ns} being the non-Sudakov form factor. The consistency constraint is given by [6] (see Fig. 1):

$$q_t^2 < \frac{(1-z)k_t^2}{z} \tag{3}$$

2 Evolution

Since the CCFM evolution cannot be easily written in an analytic closed form, a Monte Carlo method, based on [10, 11], is used. However, the Monte Carlo solution is time consuming, and cannot be used in a straightforward way in a fit program. For a realistic solution, first a kernel $\tilde{\mathcal{A}}(x'', k_t, p)$ is determined from the MC solution of the CCFM evolution equation, and then is folded with the non-perturbative starting distribution $\mathcal{A}_0(x)$:

$$x\mathcal{A}(x, k_t, p) = x \int dx' \int dx'' \mathcal{A}_0(x) \tilde{\mathcal{A}}(x'', k_t, p)\, \delta(x' \cdot x'' - x) \quad (4)$$

$$= \int dx' \int dx'' \mathcal{A}_0(x) \tilde{\mathcal{A}}(x'', k_t, p)\, \frac{x}{x'} \delta(x'' - \frac{x}{x'}) \quad (5)$$

$$= \int dx' \mathcal{A}_0(x') \cdot \frac{x}{x'} \tilde{\mathcal{A}}\left(\frac{x}{x'}, k_t, p\right) \quad (6)$$

The kernel $\tilde{\mathcal{A}}$ includes all the dynamics of the evolution, Sudakov form factors and splitting functions and is determined in a grid of $50 \otimes 50 \otimes 50$ bins in x, k_t, p.

The calculation of the cross section according to eq.(1) involves a multidimensional Monte Carlo integration which is time consuming and suffers from numerical fluctuations, and cannot be used directly in a fit procedure involving the calculation of numerical derivates in the search for the minimum. Instead the following procedure is applied:

$$\sigma_r(x, Q^2) = \int_x^1 dx_g \mathcal{A}(x_g, k_t, p) \hat{\sigma}(x, x_g, Q^2) \quad (7)$$

$$= \int dx_g\, dx'\, dx'' \mathcal{A}_0(x') \tilde{\mathcal{A}}(x'', k_t, p) \cdot \hat{\sigma}(x, x_g, Q^2) \cdot \delta(x'\, x'' - x_g) \quad (8)$$

$$= \int dx'\, dx'' \mathcal{A}_0(x') \cdot \tilde{\mathcal{A}}(x'', k_t, p) \cdot \hat{\sigma}(x, x'\, x'', Q^2) \quad (9)$$

$$= \int_x^1 dx' \mathcal{A}_0(x') \cdot \int_{x/x'}^1 dx'' \tilde{\mathcal{A}}(x'', k_t, p) \cdot \hat{\sigma}(x, x'\, x'', Q^2) \quad (10)$$

$$= \int_x^1 dx' \mathcal{A}_0(x') \cdot \tilde{\sigma}(x/x', Q^2) \quad (11)$$

Here, first $\tilde{\sigma}(x', Q^2)$ is calculated numerically with a Monte Carlo integration on a grid in x for the values of Q^2 used in the fit. Then the last step (i.e. eq.(11)) is performed with a fast numerical gauss integration, which can be used in standard fit procedures.

The fit to the HERA structure function measurements is performed applying the `herafitter` program [1, 12, 13] to determine the parameters of the starting distribution $\mathcal{A}_0$ at the starting scale Q_0:

$$x\mathcal{A}_0(x, k_t) = N x^{-B_g} \cdot (1 - x)^{C_g} (1 - D_g x) \quad (12)$$

3 Fit to HERA structure function

The parameters N, B_g, C_g, D_g in eq.(12) are determined from a fit to the combined structure function measurement [1] in the range $x < 0.01$ and $Q^2 > 5$ GeV. In addition to the gluon

induced process $\gamma^* g^* \to q\bar{q}$ the contribution from valence quarks is included via $\gamma^* q \to q$ using a CCFM evolution of valence quarks as described in [14]. The results presented here are obtained with the `herafitter` package, treating the correlated systematic uncertainties separately from the uncorrelated statistical and systematic uncertainties. To obtain a reasonable fit to the structure function data, the starting scale Q_0 as well as Λ_{qcd} has been varied. An acceptable χ^2/ndf could only be achieved when applying the consistency constraint eq.(3): without consistency constraint the best $\chi^2/ndf \sim 14 - 28$, depending on which form of the splitting function is used. With consistency constraint and the splitting function eq.(2) the best fit gives $\chi^2/ndf \sim 1.5$ for $Q_0 = 1.8$ GeV and $\Lambda_{qcd} = 0.17$ GeV at $n_f = 4$ flavours. It has been checked, that the χ^2/ndf does not change significantly when using 3 instead of 4 parameters for the initial starting distribution $\mathcal{A}_0$.

In fig.2 the resulting unintegrated gluon density **JH-set0** is shown for 2 values of p^2 compared to **set A0** [15].

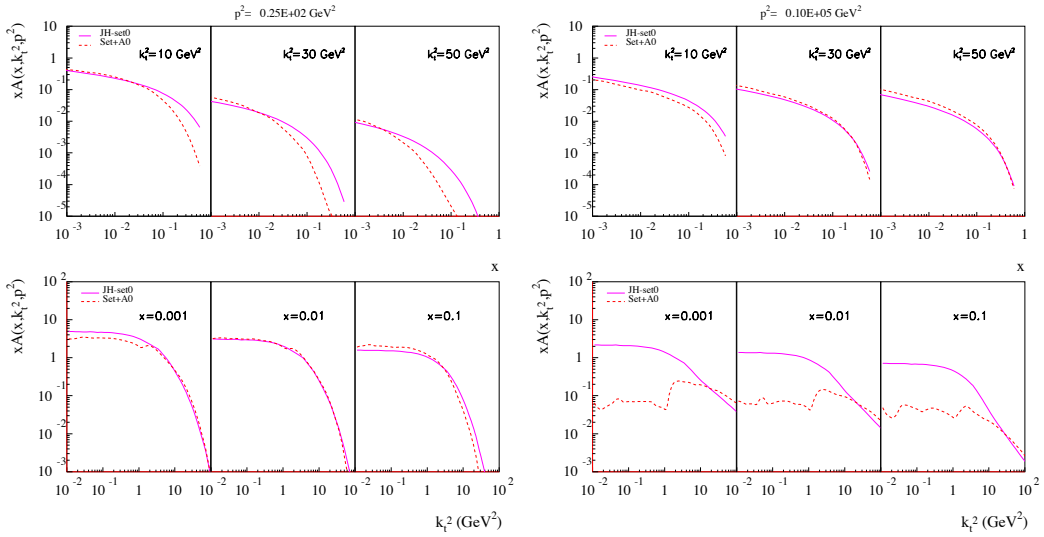

Figure 2: Unintegrated gluon density **JH-set0** for $p^2 = 25$ GeV^2 (left) and $p^2 = 10^5$ GeV^2 (right) as a function of x for different values of k_t^2 and as a function of k_t^2 for different values of x compared to **set A0** [15]

The uncertainties of the pdf are obtained within the `herafitter` package from a variation of the individual parameter uncertainties following the procedure described in [16] applying $\Delta\chi^2 = 1$. The uncertainties on the gluon are small (much smaller than obtained in standard fits), since only the gluon density is fitted. The uncertainty bands for the gluon density are shown in fig. 3(left). In fig. 3(right) the prediction for b-jet cross section as calculated from CASCADE [5] using the gluon density described here (labeled as **set0**) is shown together with a prediction using an older set (labeled as **setA 0** [15]) in comparison with a measurement from CMS [17].

Acknowledgments. We thank the conveners for the invitation and excellent organization of the meeting.

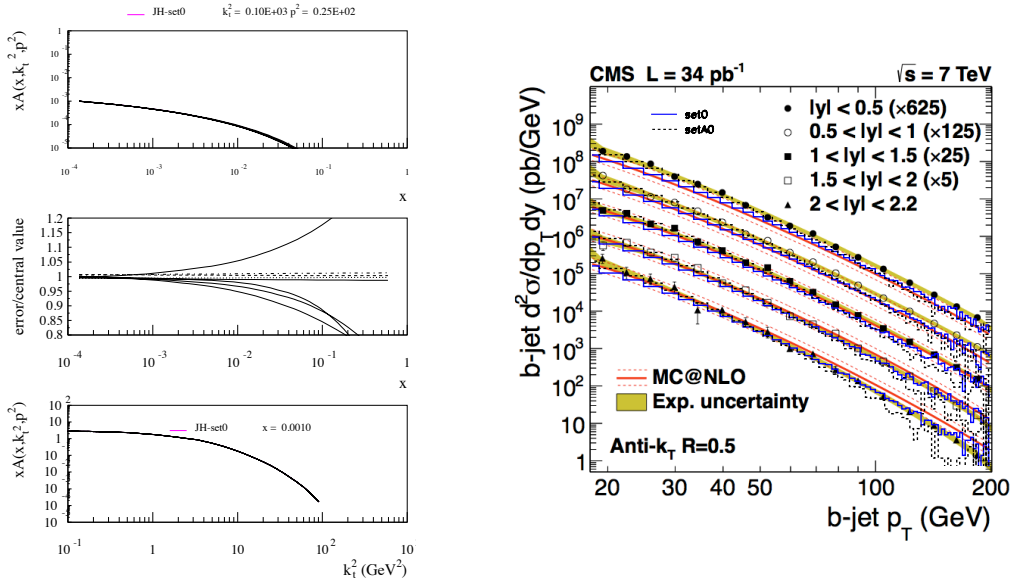

Figure 3: (left): Uncertainties of the uPDF at $p^2 = 25$ GeV^2. (right): Cross section of b-jet production as a function of p_t for different bins in y as measured by CMS [17] compared to predictions from CASCADE [5] using the unintegrated gluon density described here

References

[1] F. Aaron *et al.* JHEP **1001** (2010) 109, arXiv:0911.0884 [hep-ex]. 61 pages, 21 figures.

[2] H. Jung. Acta Phys. Polon. **B33** (2002) 2995–3000, arXiv:hep-ph/0207239.

[3] M. Hansson and H. Jung. arXiv:hep-ph/0309009.

[4] S. Catani, M. Ciafaloni, and F. Hautmann. Nucl. Phys. **B366** (1991) 135.

[5] H. Jung, S. Baranov, M. Deak, A. Grebenyuk, F. Hautmann, *et al.* Eur.Phys.J. **C70** (2010) 1237, arXiv:1008.0152 [hep-ph].

[6] J. Kwiecinski, A. D. Martin, and P. Sutton. Z.Phys. **C71** (1996) 585, arXiv:hep-ph/9602320 [hep-ph].

[7] M. Ciafaloni. Nucl. Phys. **B296** (1988) 49.

[8] B. Andersson, G. Gustafson, and J. Samuelsson. Nucl.Phys. **B467** (1996) 443. Revised version.

[9] B. Andersson *et al.* Eur. Phys. J. **C25** (2002) 771, arXiv:hep-ph/0204115.

[10] G. Marchesini and B. R. Webber. Nucl. Phys. **B349** (1991) 617.

[11] G. Marchesini and B. R. Webber. Nucl. Phys. **B386** (1992) 215.

[12] F. Aaron *et al.* Eur.Phys.J. **C64** (2009) 561, arXiv:0904.3513 [hep-ex]. 35 pages, 10 figures.

[13] "HERAFitter", 2012. http://herafitter.hepforge.org/.

[14] M. Deak, F. Hautmann, H. Jung, and K. Kutak. arXiv:1012.6037 [hep-ph].

[15] H. Jung. arXiv:hep-ph/0411287.

[16] J. Pumplin, D. Stump, R. Brock, D. Casey, J. Huston, *et al.* Phys.Rev. **D65** (2001) 014013, arXiv:hep-ph/0101032 [hep-ph].

[17] S. Chatrchyan *et al.* JHEP **1204** (2012) 084, arXiv:1202.4617 [hep-ex].